applied sciences

MDPI

Article

Exergy Analysis of Air-Gap Membrane Distillation Systems for Water Purification Applications

Daniel Woldemariam [1,2,*], Andrew Martin [1] and Massimo Santarelli [1,2]

[1] Energy Technology Department, KTH Royal Institute of Technology, Brinellvägen 68, SE-100 44 Stockholm, Sweden; andrew.martin@energy.kth.se (A.M.); massimo.santarelli@polito.it (M.S.)

[2] Department of Energy (DENERG), Politecnico di Torino, PoliTo, Corso Duca degli Abruzzi 24, 10129 Turin, Italy

* Correspondence: dmwo@kth.se; Tel.: +46-08-790-7477

Academic Editor: Enrico Drioli

Received: 13 December 2016; Accepted: 15 March 2017; Published: 20 March 2017

Abstract: Exergy analyses are essential tools for the performance evaluation of water desalination and other separation systems, including those featuring membrane distillation (MD). One of the challenges in the commercialization of MD technologies is its substantial heat demand, especially for large scale applications. Identifying such heat flows in the system plays a crucial role in pinpointing the heat loss and thermal integration potential by the help of exergy analysis. This study presents an exergetic evaluation of air-gap membrane distillation (AGMD) systems at a laboratory and pilot scale. A series of experiments were conducted to obtain thermodynamic data for the water streams included in the calculations. Exergy efficiency and destruction for two different types of flat-plate AGMD were analyzed for a range of feed and coolant temperatures. The bench scale AGMD system incorporating condensation plate with more favorable heat conductivity contributed to improved performance parameters including permeate flux, specific heat demand, and exergy efficiency. For both types of AGMD systems, the contributions of the major components involved in exergy destruction were identified. The result suggested that the MD modules caused the highest fraction of destructions followed by re-concentrating tanks.

Keywords: exergy; energy; membrane distillation; specific heat; entropy; efficiency

1. Introduction

Exergy studies on membrane-based desalination and water purification technologies such as reverse osmosis (RO) and membrane distillation (MD) focus on evaluating the exergetic efficiencies of the components, mainly membrane modules. Unlike energy, exergy is destroyed and can only be conserved when all processes occurring in a system and its surrounding environment are reversible [1]. This thermodynamic irreversibility in a system can be quantified and referred to as exergy destruction. Therefore, the exergy efficiency of processes is a measure of their approach to ideality or reversibility [2]. The exergy rates in streams of processes associated with heat transfer such as MD depend mainly on the temperature at which the process occurs in relation to the temperature of the environment. The exergy efficiencies of such processes are dependent on heat recovered and heat losses through module surfaces to the surrounding atmosphere. Hence, exergy analysis provides unique insights into the types, locations, and causes of losses and aids in identifying improved thermal integration.

Membrane distillation involves the separation of water from a preheated feed by subjecting it to phase change and the subsequent passage through a hydrophobic porous membrane to yield pure water upon condensation. Membrane distillation requires heat to evaporate the feed and electricity for the low pressure pumps. The heat sources used in MD include solar [3–7], district heat [8], or waste heat [9,10]. Though low-grade heat is sufficient to drive the MD process, thermal energy demand is

high, and this together with low permeate flux create challenges for the technology. The high heat demand is largely related to the substantial amount of heat transferred through the membrane, mainly as latent heat but partially also from conductive heat transfer. However, the ability to supply an ultra high-quality permeate together with the possibility to drive the MD process with low grade or waste heat are the opportunities gaining acceptance in large scale industrial applications.

Exergy analyses of membrane-based desalination or water purification processes have been investigated by few researchers. Banat and Jwaied [4] conducted exergy destruction analyses for compact and large-scale solar-powered MD systems. They reported that most of the exergy destruction was in the MD modules with 98.8% and 55.14% for compact and large scale systems, respectively. Exergy efficiency of a 24,000 m^3/day DCMD desalination plant operated with and without heat recovery system was reported as 28.3% and 25.6% for the desalination plant with and without heat recovery, respectively [11]. They also reported energy consumptions of 39.7 kWh/m^3 and 45 kWh/m^3 for the same plant with and without heat recovery, respectively.

Another study [12] on energetic and exergetic analysis of RO/MD and NF/RO/MD hybrid systems for production capacities of 904 and 836 m^3/h, respectively, reported specific thermal energy demand ranging from 2.25 to 15 kWh/m^3. The exergy destructions due to entropy production for each hybrid system was reported in the range of 7300 to 15,100 MJ/h. Macedonio and Drioli carried out an energetic, exergetic, and economic evaluation of seawater desalination [13]. The integrated system consisted of microfiltration, nanofiltration, membrane crystallization (MCr), RO, and MD, where MCr was applied on NF retentate, and MD was applied on RO retentate. Without energy recovery, the specific energy demand (SED) was found to be 28 kWh/m^3. When a pressure exchanger is included as an energy recovery device, a slightly lower SED (27.5 kWh/m^3) was obtained. The reported exergetic efficiencies ranged from 15.8% without energy recovery to 21.9% when including the pressure exchanger and internal heat recovery. Sow et al. [14] analyzed solar-driven distillers and reported exergy efficiencies of 19%–26%, 17%–20%, and less than 4% for triple-effect, double-effect, and single-effect systems. Garcia-Rodriguez and Gomez-Cmacho [15] analyzed exergetic efficiencies of a 14-cell multi-effect distillation (SOL-14 MED) plant in Plataforma Solar de Almeria, Spain. They developed a thermodynamic computer program in order to propose improvements. The reported results showed that exergy efficiency of the plant increases from 1.4% to 4.7% and from 14.3% to 25.7% because of the integration of a double-effect absorption heat pump and energy recovery, respectively.

Thermal energy demands have been analyzed for membrane-based water desalination systems. Solar powered MD was reported to have a specific heat demand of 140–200 kWh/m^3 [6], whereas a solar thermal and PV integrating stand-alone MD plant was reported to have a heat demand of 200–300 kWh/m^3 [16]. Islam et al. analyzed exergy destructions in different components of a two-stage 553 m^3/h capacity reverse osmosis unit in a thermal power plant. The reported contributions for exergy destructions showed a maximum exergy loss in throttling valves (57%) followed by RO modules (21%), with plant's overall second-law efficiency of 4.1% [17]. Energy (first-law) analysis is widely used for assessing efficiencies of water desalination systems. However, as it does not account for the quality of energy considered, second-law analysis is required to decide how much of the available energy is destroyed, for example, in heat exchangers and MD modules. Exergy analysis also helps to identify components responsible for deterioration of the available energy in terms of exergy destruction and hence helps to suggest unit redesign. It is clear that MD modules are responsible for the majority of the exergy destruction in water purification or desalination systems employing this technology. The challenges to be achieved in this study that have not been addressed previously are summarized in the following questions: What is the exergy destruction contribution of each component of AGMD system? How would temperature difference across the module affect the exergy efficiency of the modules? What would the applications for water purification be It was believed that the answers to these questions would be useful for developing or redesigning large-scale MD modules with improved exergy performances. Indeed, temperature dependency on exergy efficiency and exergy destruction is a key parameter, since MD technology offers freedom in selecting heat source and

heat sink temperatures when integrated with other processes. Such aspects have not been covered in sufficient detail in previous studies. Moreover, to the authors' knowledge, air gap membrane distillation (AGMD) has not been previously considered in this context.

The main objective of this study was to evaluate the exergy efficiencies and destruction of AGMD systems. The analyses are based on two types of semi-commercial AGMD modules for a new application of water treatment where contaminants in the feed are at relatively low concentrations. The study covers calculations of the exergy destruction contributions of the components of each MD system considered. Additionally, effects of feed–coolant temperature differences are analyzed, and comparisons are made with other studies on similar and related water purification systems.

2. Materials and Methods

Thermodynamic properties of streams used for the calculation of exergy analyses were obtained from testing two AGMD modules, Xzero and Elixir500 at IVL Hammarby Sjöstadsverk and KTH, respectively. Both modules have identical membrane materials of PTFE with PP backing but differ in the total membrane area and the nature of the condensation surface. The Xzero unit was originally intended for industrial applications such as semiconductor fabrication facilities (fabs), whereas the Elixir500 unit was designed for small-scale water purification. The Xzero module utilizes PP plates and the Elixir500 module employs a thin plate of stainless steel condensation surface, the same design as plate-and-frame heat exchangers. Both MD modules are assembled and supplied by Scarab Development AB. More information on these modules can be found in the literature [8,18].

2.1. Experimental Setup for the Pilot AGMD System

The pilot MD system analyzed in this study consists of 10 AGMD modules arranged in five cascades, each containing two modules connected in series. Figure 1 shows the photograph of the pilot MD system. The AGMD system is connected to the district heating network through heat exchangers, which supply the heat required to heat up the MD feed. The major components include the AGMD modules, the recirculation tank with a 1 m^3 capacity, and an expansion tank for pressure balancing on the coolant side. Two plate and frame heat exchangers (nominal capacity of 300 kW, working temp. of 0–170 °C) and two pumps (each 2.2 kW power demand at Q_{max} = 17 m^3/h and H_{max} 28.7 m pressure head) are also connected.

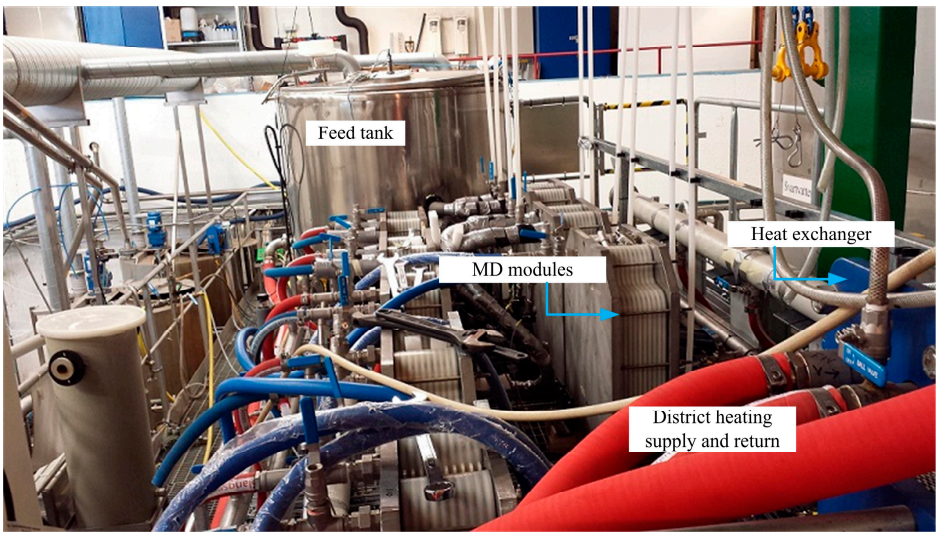

Figure 1. Xzero Pilot air gap membrane distillation system at Hammarby Sjöstadsverk testing and demonstration facility, Stockholm, Sweden.

An illustration of the pilot plant depicting all the streams involved is shown in Figure 2. Each MD module is constructed from a stack of 10 cassettes, each containing two membranes with a combined area of 0.28 m^2. The membrane characteristics are a 0.2 mm thickness, a 0.2 µm average pore size, and an 80% porosity. The size of one module is 63 cm wide and 73 cm high, with a stack thickness of 17.5 cm. During the experiments, data was logged for parameters connected to the control system. PT100 thermocouples (range: −50 °C–200 °C, accuracy: ±4 °C) installed close to the MD module's inlet and outlet streams were used to measure temperatures. FLEX-F flow sensors (linear flow range: 2–150 cm/s, accuracy: ±10 cm/s) were used to measure the flow rates of streams, which were recorded by the control system. System control and data (temperature, pressure, and the flow rates of the feed and cooling water) were registered on a personal computer with Citect Runtime SCADA software installed. A YOKOGAWA DC402G dual cell conductivity analyzer (ranges of detection 1 µS/cm–25 mS/cm and accuracy of ±0.5%) was introduced to monitor the conductivity of the product water.

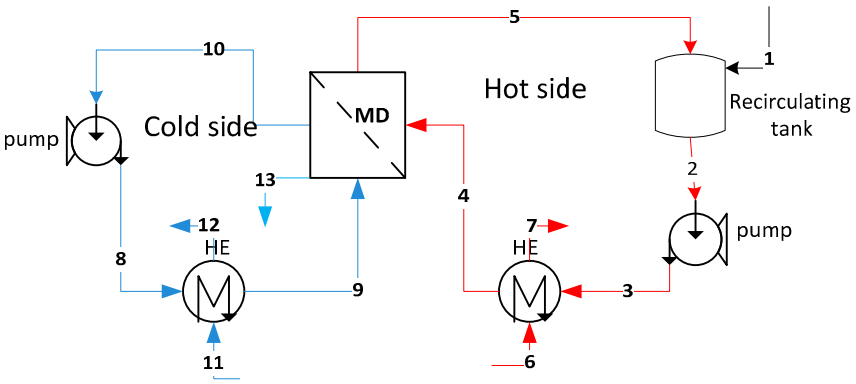

Figure 2. The Xzero AGMD unit used and the different streams considered.

2.2. Experimental Setup for Bench Scale AGMD

The bench scale AGMD module includes a thin plate of stainless steel inserted as a condensation plate, an effective membrane area of 0.19 m^2, with an 80% porosity and a 0.2 mm thickness. Figure 3 shows a photograph of the Elixir500 lab unit tested at KTH.

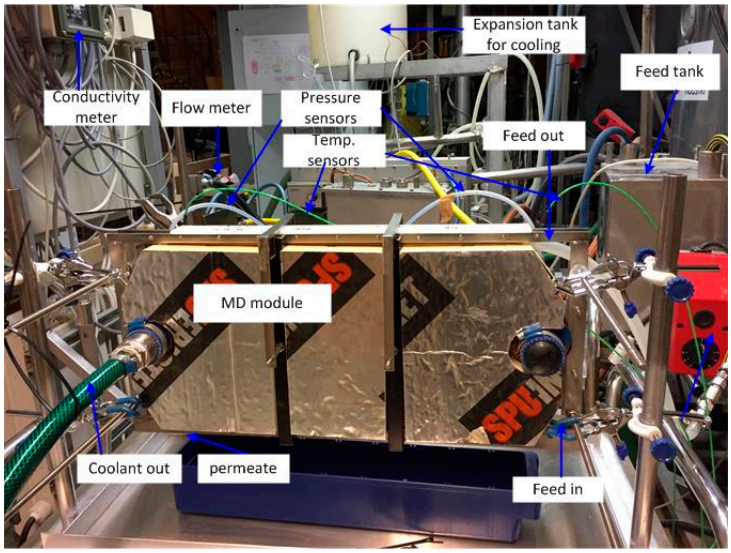

Figure 3. Bench scale Elixir500 AGMD test unit at KTH Royal Institute of Technology, Energy Department laboratory.

In Figure 4, the schematic diagram shows the main components and water streams (1–8) considered during analyses. The red lines show streams on the hot feed side of the module and the blue lines for the streams on the cooling side. Stream 8 refers to the permeate collected from the module. The bench scale MD unit consists of one MD unit module, a 20 L capacity heating, a recirculating tank, two pumps for each of the coolant, and feed streams. Two heaters immersed in the tank with a combined heating rate of 4.5 kW provide temperature control for the feed water.

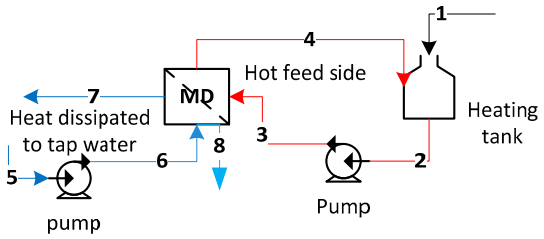

Figure 4. Water and heat streams considered in the Elixir500 AGMD lab unit.

The obtained permeate was returned to the feed tank so that feed concentration would be constant over the course of experimentation. In order to measure the feed and cold-side temperatures, thermocouples were installed at the inlets and outlets of the module and were connected to a data logger (Keithley 2701 DMM with a 7706 card). Once-through tap water was used as a heat sink, which exchanges heat with an external water to vary coolant temperature. Rotameters with built-in control valves measured feed and coolant water flow rates. Product water was measured with a graduated cylinder and stopwatch, typically during a 30 min period of steady operation.

The reference state and experimental conditions are given in Table 1. Data for the exergy analysis is taken for one cascade of MD modules containing two modules connected in series. Pressure drops across the MD modules are very low—less than 0.019 MPa. The concentration of total dissolved solutes in the feed water is also relatively low in comparison to seawater desalination applications (two orders of magnitude or less). As the three different cases have different feed and cooling temperatures, the exergy rates will be mainly affected by them.

Table 1. The experimental and reference state conditions for the two types of AGMD systems tested.

Property	Value	
	Xzero	**Elixir500**
Reference temperature, K	288	
Reference pressure, MPa	0.1	
Membrane area, m^2	4.6	0.19
Feed rate, L/min	20	3.8
Coolant rate, L/min	20	1.9
Feed temperature, K	353	338–353
Coolant temperature, K	288–328	
TDS of feed and coolant, g/L	0.25	0.36

2.3. Exergy Analysis Methods

The exergy rates of each stream throughout the MD systems and the exergy efficiencies of the MD modules are analyzed by taking the basic exergy definitions [1] and relationships for MD models as reported in the literature [5,6,9]. The intensive parameters governing the MD process are temperature and composition, and exergies related to kinetic and potential are not considered. Hence, the exergy rate is the sum of the physical and chemical exergies of streams as given by Equation (1).

$$Ex = Ex_{ph} + Ex_{ch} \quad (1)$$

Ex_{ph} represents the thermomechanical exergy based on the temperature of the stream, and Ex_{Ch} refers to the chemical exergy from the chemical potentials of the solute components in the stream. The physical exergy can be expressed in terms of heat enthalpies and entropies at the specified condition (h, s) and reference condition (h_o, s_o) by Equation (2).

$$Ex_{ph} = (h - h_o) - T_o \times (s - s_o) \quad (2)$$

The individual exergies due to pressure and temperature are calculated independently and sum up to the physical exergy. Even though the working pressure in MD is generally very low, its effect could be detected in exergy destruction calculations due to pressure changes, especially in series configured modules. These pressure and temperature related exergies are given as follows, in Equations (3) and (4) [5,10].

$$Ex_p = \dot{m} \times (p - p_o)/\varrho \quad (3)$$

$$Ex_T = \dot{m} \times c_p \times [(h - h_o) - T_o(s - s_o)] \quad (4)$$

Chemical exergy based on the chemical potentials or concentrations (C) of the components in the stream is calculated as in Equation (5).

$$Ex_c = -\dot{m} \times N_s \times R \times T_o \times \ln X_s \quad (5)$$

$$\text{where } N_s = (1000 - \sum C_i/\varrho)/MW_s \quad (6)$$

$$\text{and } Xs = N_s/[N_s + \sum(\beta_i \times C_i/\varrho \times MW_i)] \quad (7)$$

The exergy change across the MD module or any other component of the MD system is calculated from the differences in inlet and outlet exergies as

$$\Delta Ex = \sum Ex_{in} - \sum Ex_{out} \quad (8)$$

The second-law efficiency of the MD system is the ratio of the minimum exergy input required (which is equivalent to the minimum work of separation) to the total actual exergy input:

$$\eta(\%) = (W_{min}/E_{xin}) \times 100 \quad (9)$$

The minimum work input required for the MD process is the difference between outgoing and incoming total exergies of the hot stream:

$$W_{min} = Ex_{permeate} + Ex_{feed\ out} - Ex_{feed\ in} \quad (10)$$

The exergy destruction due to irreversibility in the process is calculated by subtracting exergy determined from the second-law entropy generation [1] according to the Gouy–Stodola formula:

$$Ex_{dest} = S_{gen} \times T_o \quad (11)$$

where T_o is the reference temperature, and S_{gen} is the entropy generated due to irreversibility of the process, given as

$$S_{gen} = \Delta S_{total} = \Delta S_{source} + \Delta S_{sink} = Q_{source}/T_{source} + Q_{sink}/T_{sink} \quad (12)$$

where the Q_{source} and Q_{sink} represent the heat lost and gained from the heat source and sink, respectively.

The electrical exergy input for the pumps is

$$Ex_{el} = \dot{m} \times \Delta P/(1000 \times \eta_p) \quad (13)$$

where ΔP is the pressure head in Pa and η_p is for pump efficiency. The exergy of electric power involved for the pumps is equal to the energy and taken as pure exergy.

For simplicity, the exergy destroyed can be expressed as a percentage as related to the exergy input:

$$\varepsilon\% = Ex_{dest}/Ex_{in} \quad (14)$$

Ex_{dest}% of a component is then calculated the fraction of exergy destruction by the particular component in comparison to the total destroyed exergy,

$$Ex_{dest}\% = \frac{Ex_{dest\ i}}{Ex_{dest\ total}} \quad (15)$$

where $Ex_{dest\ i}$ is the exergy destroyed in component i, and $Ex_{dest\ total}$ is the total exergy destroyed in the MD system.

3. Results and Discussion

Exergy Efficiency of the AGMD Modules

Results from the permeate production rates for the two types of AGMD units are summarized in Figure 5 in terms of kilogram per square meter of membrane per second (kg/m^2s). The flux decreases as the temperature difference decreases across the MD module, which is due to the decline in the rate of condensation and concomitant drop in transmembrane transport of vapor across the membrane as the temperature difference decreases. Higher specific heat demands accompany this increase in permeate flux with increasing ΔT. The lower feed temperature condition generally shows a lower permeate flux, as observed for Xzero module's performance at 65 °C and 80 °C. When fluxes from the two MD modules are compared, the flux from Elixir500 MD unit is nearly three times higher than that from the Xzero MD unit at the same feed temperature and ΔT (65 °C).

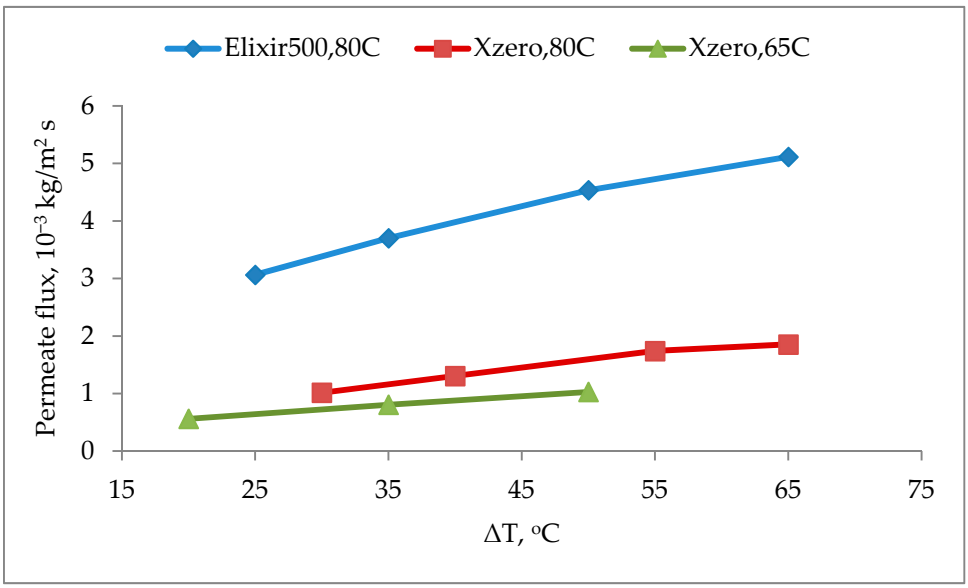

Figure 5. Permeate flux of Xzero and Elixir500 AGMD systems regarding permeate flux for different temperature differences at feed temperatures of 80 °C and 65 °C.

The other thermodynamic performance parameters: exergy efficiency, exergy destruction, and specific heat input are summarized for both modules in Figures 6 and 7. For both modules types, exergy efficiency improves when the feed–coolant temperature difference goes up. For the Xzero unit at a feed of 80 °C, exergy efficiency more than doubled as ΔT increased from 30 °C to 65 °C. This

increase is linked to the improved heat recovery at the heat sink for a higher ΔT. This is evidently observed from the decrease in exergy destruction at a higher ΔT compared to lower levels (Figure 7). The trend is similar for both feed temperatures of 80 °C and 65 °C. However, the lower feed temperature condition generally shows lower exergy efficiency and higher exergy destruction when compared to the corresponding performance at higher feed temperatures. For this MD unit, it can be said that a higher feed temperature and ΔT favor higher flux and exergy efficiency and lower exergy destruction than lower ΔT cases, of course at the expense of additional specific heat demand.

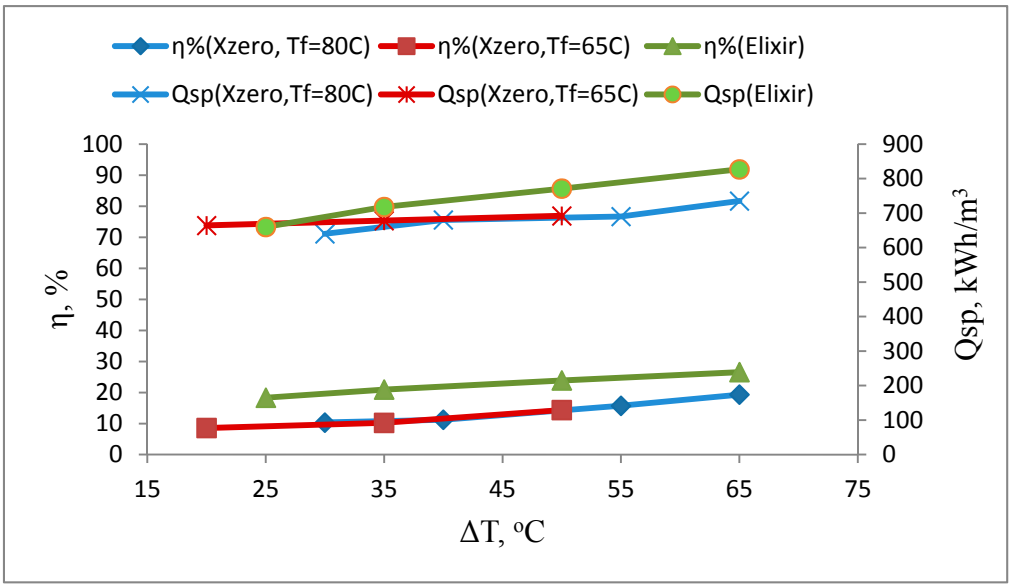

Figure 6. Performance of Xzero and Elixir500 AGMD systems regarding exergy efficiency and specific heat demand at different feed–coolant temperature differences for fixed feed temperatures of 80 °C (for both modules) and 65 °C (only for Xzero).

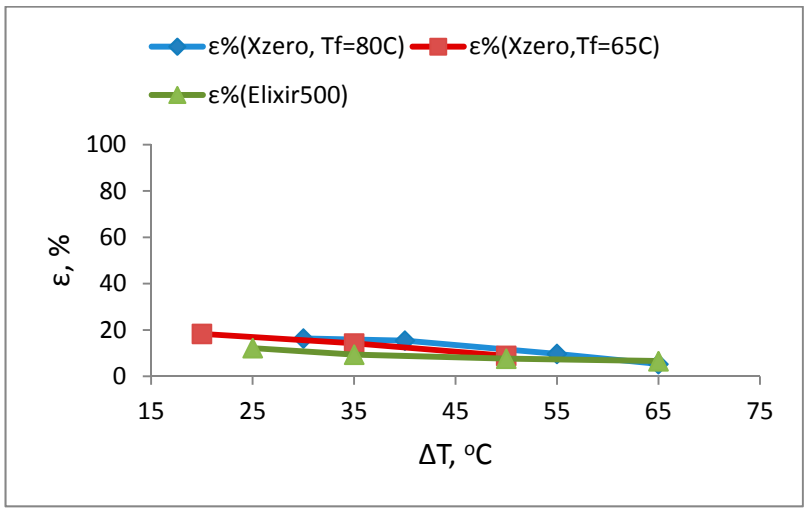

Figure 7. Exergy destructions and specific heat demand at different feed–coolant temperature differences for fixed feed temperatures of 80 °C (for both modules) and 65 °C (only for Xzero).

Similarly, for the bench scale AGMD unit, the general trend in the performances with a change in ΔT is the same as that of the results from the pilot-scale AGMD system. The effect of improved condensation in the Elixir500 module is reflected in the higher specific heat input owing to the higher heat transfer across the module. Hence, higher exergy efficiency and lower exergy destruction is

achieved for the Elixir500 unit as compared to the Xzero module. The lower specific heat demand for the Xzero module results from the reduced heat transfer across the condensation plate in comparison to the other module, though the Xzero showed severe heat losses from the frames and cover to the surrounding atmosphere by free convection [8]. For both types of MD systems, it is evident that a lower temperature difference across the module reduces performance, including the permeate flux and exergy efficiency.

As the pressure drop across the AGMD modules is low (0.01 to 0.02 MPa) and mass balance is achieved across the MD unit, exergy losses from pressure and concentration changes are not significant. Hence, the major contributor to the exergy destruction is the heat loss from the modules to the surroundings and the latent heat transferred with the permeate. The heat transfer rates across the module can be assisted by employing condensation plates with good heat conduction, minimizing heat losses to the module frames and covers, and using membranes of lower heat conduction properties.

Considering each component of the MD system as open, the exergy destruction contributions can be pinpointed. Doing so will enable system designers to optimize the performance of the components. The result from calculations of exergetic destruction contributions of each component from both MD systems is summarized in Figure 8. The maximum fraction of exergy destruction in both MD types comes from the MD modules. However, the percentage is higher for the Xzero module (58%) than for the Elixir500 (43%). The pumps are in both cases the lowest contributors of exergy destruction. The re-concentrating tank contributed 34% of the exergy destruction to the Elixir500 unit, which was caused by the heat losses through the steel wall and evaporation occurred through openings in the cover as source of heat was electric heaters. Even though in both types of MD modules it is found that the MD modules contribute the highest exergy destruction, the Elixir500 modules showed a lower percentage than those of the Xzero. The lower percentage of exergy destruction for the Elixir500 MD module is mainly due to the improved heat transfer capability of the condensation plates used and hence the higher degree of heat recovery from the cooling side of the module.

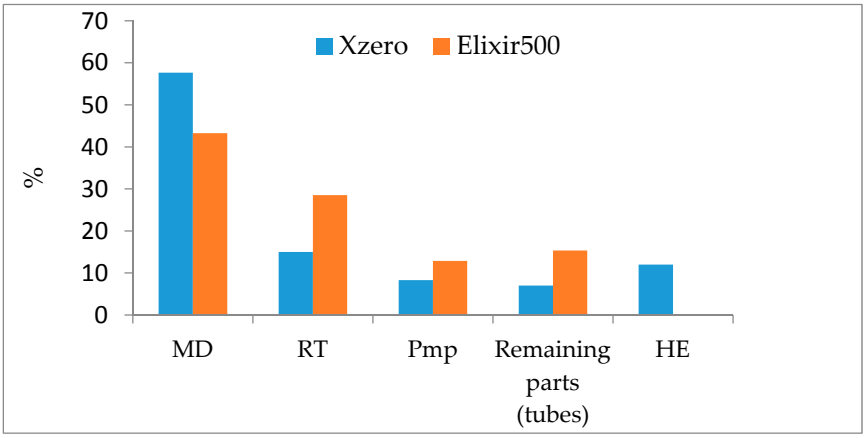

Figure 8. Percentage contribution of exergy destruction from the different components of each AGMD system.

A literature search for exergy efficiency analyses for related water purification processes, such as RO, revealed wide discrepancies in the values. Table 2 summarizes exergy efficiency for some of the standalone and integrated processes. In contrast to MD, the majority of the exergy rates in RO are derived from the high pressures involved, i.e., 15–25 bars for brackish water and 60–80 bars for seawater, hence the related pressure drop as reflected in improved efficiencies when a pressure exchanger is considered [19]. The very low exergy efficiency of MD reported [4] was from the one powered by solar, and the high exergy losses were due to the MD and heat exchanger units. The MD units' exergy efficiency values are relatively closer to each other than with RO. If we make comparisons

between systems of similar processes and capacities, we see, for example, that the MD with a capacity of 0.3 m^3/day [4] and Elixir500 from the present study have comparable exergy efficiency.

Table 2. Summary of exergy efficiencies for different MD configurations and RO from the literature.

Process	Capacity, m^3/Day	Exergy Efficiency, %	Reference
RO	7250	4.3	[20]
RO	2850	0.72	[21]
SWRO	7586	5.82	[22]
MF-NF-RO	12,408	30.9	[23]
MD on RO retentate	22,344	19.1–21.9	[23]
MD	0.31	0.3	[4]
DCMD with HR	24,000	28.3	[11]
DCMD without HR	24,000	25.6	[11]
AGMD (Xzero)	0.22–0.73	8.54–19.32	(This study)
AGMD (Elixir500)	0.1–0.17	18.3–26.5	(This study)

4. Concluding Remarks

The exergy efficiency analyses that were carried out on pilot scale and bench MD systems illustrate the performance of the separation technologies based on useful energy, i.e., exergy. The AGMD systems tested showed different exergy efficiencies mainly due to the differences in module size and the type of condensation plates used. The exergy efficiencies were also affected to different degrees by the feed–coolant temperature differences in both types of modules. For the Xzero MD module, the exergy efficiency was not significantly affected by the difference in temperature across the module, whereas, for Elixir, a higher temperature difference across the module yielded higher exergy efficiencies and lower exergy destruction. The exergy efficiency results showed that the materials selection of the condensation plate plays a role in optimizing the performance of MD systems. This is clearly an important part of the MD system design and optimization, as the MD module contributes to the majority of the exergy destruction. Materials that could be considered for optimum heat transfer across modules and hence less exergy destruction from MD modules include stainless steel and high density polyethylene, which have better thermal conductivities than polypropylene. The selection of membrane and support material should also be considered when designing MD modules, as membrane and support materials, unlike condensation plates, should have less thermal conductivity for better thermal efficiency of modules.

Acknowledgments: This research has been done in collaboration with KTH Royal Institute of Technology, and Politecnico di Torino, PoliTo funded through Erasmus Mundus Joint Doctoral Program SELECT+, the support of which is gratefully acknowledged.

Author Contributions: Daniel Woldemariam conceived, designed, and performed the experiments; all three authors analyzed the data; and Daniel Woldemariam composed the article under the guidance of the co-authors.

Conflicts of Interest: The authors declare no conflict of interest. The funding sponsors had no role in the design of the study; in the collection, analyses, or interpretation of data; in the writing of the manuscript; or in the decision to publish the results.

References

1. Tsatsaronis, G. Definitions and nomenclature in exergy analysis and exergoeconomics. *Energy* **2007**, *32*, 249–253. [CrossRef]
2. Tsatsaronis, G. Thermoeconomic analysis and optimization of energy systems. *Prog. Energy Combust. Sci.* **1993**, *19*, 227–257. [CrossRef]
3. Guillén-Burrieza, E.; Blanco, J.; Zaragoza, G.; Alarcón, D.-C.; Palenzuela, P.; Ibarra, M.; Gernjak, W. Experimental analysis of an air gap membrane distillation solar desalination pilot system. *J. Membr. Sci.* **2011**, *379*, 386–396. [CrossRef]

4. Banat, F.; Jwaied, N. Exergy analysis of desalination by solar-powered membrane distillation units. *Desalination* **2008**, *230*, 27–40. [CrossRef]
5. Koschikowski, J.; Wieghaus, M.; Rommel, M.; Ortin, V.S.; Suarez, B.P.; Betancort Rodríguez, J.R. Experimental investigations on solar driven stand-alone membrane distillation systems for remote areas. *Desalination* **2009**, *248*, 125–131. [CrossRef]
6. Koschikowski, J.; Wieghaus, M.; Rommel, M. Solar thermal driven desalination plants based on membrane distillation. *Desalination* **2003**, *156*, 295–304. [CrossRef]
7. Khayet, M. Solar desalination by membrane distillation: Dispersion in energy consumption analysis and water production costs (a review). *Desalination* **2013**, *308*, 89–101. [CrossRef]
8. Woldemariam, D.; Kullab, A.; Fortkamp, U.; Magner, J.; Royen, H.; Martin, A. Membrane distillation pilot plant trials with pharmaceutical residues and energy demand analysis. *Chem. Eng. J.* **2016**, *306*, 471–483. [CrossRef]
9. Dow, N.; Gray, S.; Li, J.; Zhang, J.; Ostarcevic, E.; Liubinas, A.; Atherton, P.; Roeszler, G.; Gibbs, A.; Duke, M. Pilot trial of membrane distillation driven by low grade waste heat: Membrane fouling and energy assessment. *Desalination* **2016**, *391*, 30–42. [CrossRef]
10. Jansen, A.E.; Assink, J.W.; Hanemaaijer, J.H.; van Medevoort, J.; van Sonsbeek, E. Development and pilot testing of full-scale membrane distillation modules for deployment of waste heat. *Desalination* **2013**, *323*, 55–65. [CrossRef]
11. Al-Obaidani, S.; Curcio, E.; Macedonio, F.; Di Profio, G.; Al-Hinai, H.; Drioli, E. Potential of membrane distillation in seawater desalination: Thermal efficiency, sensitivity study and cost estimation. *J. Memb. Sci.* **2008**, *323*, 85–98. [CrossRef]
12. Criscuoli, A.; Drioli, E. Energetic and exergetic analysis of an integrated membrane desalination system. *Desalination* **1999**, *124*, 243–249. [CrossRef]
13. Macedonio, F.; Drioli, E. An exergetic analysis of a membrane desalination system. *Desalination* **2010**, *261*, 293–299. [CrossRef]
14. Sow, O.; Siroux, M.; Desmet, B. Energetic and exergetic analysis of a triple-effect distiller driven by solar energy. *Desalination* **2005**, *174*, 277–286. [CrossRef]
15. García-Rodríguez, L.; Gómez-Camacho, C. Exergy analysis of the SOL-14 plant (Plataforma Solar de Almería, Spain). *Desalination* **2001**, *137*, 251–258. [CrossRef]
16. Banat, F.; Jwaied, N.; Rommel, M.; Koschikowski, J.; Wieghaus, M. Desalination by a "compact SMADES" autonomous solarpowered membrane distillation unit. *Desalination* **2007**, *217*, 29–37. [CrossRef]
17. Aljundi, I.H. Second-law analysis of a reverse osmosis plant in Jordan. *Desalination* **2009**, *239*, 207–215.
18. Khan, E.U.; Martin, A.R. Water purification of arsenic-contaminated drinking water via air gap membrane distillation (AGMD). *Period. Polytech. Mech. Eng.* **2014**, *58*, 47–53. [CrossRef]
19. Querol, E.; Gonzalez-Regueral, B.; Perez-Benedito, J.L. Exergy Concept and Determination. In *Practical Approach to Exergy and Thermoeconomic Analyses of Industrial Processes*; Springer: Heidelberg/Berlin, Germany, 2013; pp. 9–28.
20. Cerci, Y. Exergy analysis of a reverse osmosis desalination plant in California. *Desalination* **2002**, *142*, 257–266. [CrossRef]
21. Ameri, M.; Eshaghi, M.S. A novel configuration of reverse osmosis, humidification–dehumidification and flat plate collector: Modeling and exergy analysis. *Appl. Therm. Eng.* **2016**, *103*, 855–873. [CrossRef]
22. El-Emam, R.S.; Dincer, I.; Salah El-Emam, R.; Dincer, I.; El-Emam, R.S.; Dincer, I. Thermodynamic and thermoeconomic analyses of seawater reverse osmosis desalination plant with energy recovery. *Energy* **2014**, *64*, 154–163. [CrossRef]
23. Drioli, E.; Curcio, E.; Di Profio, G.; Macedonio, F.; Criscuoli, A. Integrating Membrane Contactors Technology and Pressure-Driven Membrane Operations for Seawater Desalination. *Chem. Eng. Res. Des.* **2006**, *84*, 209–220. [CrossRef]